PHYSICOCHEMICAL PROBLEMS
OF MATERIALS PROTECTION

Tribo-Corrosion Protection of Valves and Rotors using Cermet Layers Applied with HVOF[1]

M. J. Quintana[a], **R. Gonzalez**[a, *], **D. Fernandez**[b], **and L. F. Verdeja**[b]

[a]*Universidad Panamericana, Faculty of Engineering,
03920, Mexico*
[b]*University of Oviedo, E. T. S. de Ingenieros de Minas, 33004, Spain*
e-mail: lfv@uniovi.es, roblez@up.edu.mx

Abstract—Protection of conventional steel parts in equipment that must withstand wear of the tribo-corrosion type (combination of heat and an aqueous medium) can be achieved by High Velocity Oxy-Fuel (HVOF) techniques, applying carbide-based cermet layers which decrease tribological and corrosion mechanisms. Three different carbide layers were applied to a ferritic-pearlitic steel in order to characterize properties such as sliding friction coefficient, phase identification, adhesion to the substrate, porosity, layer thickness and wear mechanisms. An example of a real rotatory equipment after a working campaign, both with and without protective layer is presented. The capacity of the protective layer to extend the life of parts like the one analyzed is evident even if zones of the layer are detached during the campaign.

INTRODUCTION

Strategies to achieve a more rational and efficient use of raw materials in manufacturing processes have been a tendency in the last decades. The bulk materials used in the design and construction of industrial equipment must withstand wear of both mechanical and chemical (or electro-chemical) types. Furthermore, if temperature is high (above 250°C, which is a temperature limit that restricts the use of water in the liquid state), other oxidation processes are activated (oxidizing atmospheres with $P(O_2) \geq 1 \times 10^{-4}$ MPa), as well as chemical attack by metallic or metal oxides mixtures in the form of melts.

Common solutions for design problems in parts that present wear due to surfaces simultaneously exposed to mechanical impact and oxidation include increasing the thickness or hardness of the bulk material. An outdated technique was the use of thicker walls, while current solutions, used by most specialized engineering firms, are focused in the modification of materials using new alloying elements and/or heat treatments, resulting in harder materials though losing toughness. Nevertheless, an increase in hardness is not always directly related to a better tribological behavior [1].

Tribo-corrosion phenomenon is relevant in primary industrial processes, and specifically on preparation-grinding-milling of raw materials and mostly

evident in finishing stages that use aqueous environments. Likewise, digestion-lixiviation processes for pulps (solids in aqueous suspension) using acid, basic or oxidizing solutions also present this type of wear. As an example, food industry extracts sugar from beets using alkaline solutions at 50−70°C.

Protection of the surface using High Velocity Oxygen Fuel (HVOF) is one of many thermal projection techniques for surface engineering processes, in which a suspension of metallic and/or ceramic powders are sprayed, at a speed two or three times higher than sound and 1700−1900°C, on the surface of the material to be protected [2]. Piping of oil and gas industry in contact with sea water (offshore facilities) is a good example of this type of coatings [3].

THEORETICAL ANALYSIS

A system suffers mechanical wear when superficial contact with another material takes place: a force is applied and there is considerable displacement between the surfaces. If mechanical conditions or thermal variations are high, the wear may produce failure by fatigue. Another mechanism to be considered in the wear of materials in general (and metals and their alloys in particular) is electrochemical corrosion: water acting as solvent and addition of acid or basic products, along with dissolved oxygen and temperature, will activate the anodic dissolution of the metal [4].

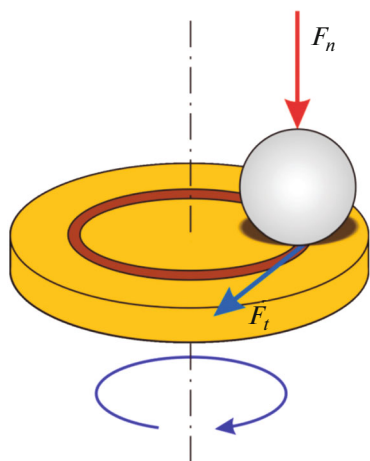
[1] The article is published in the original.

Fig. 1. Typical ball-on-disc setup where F_n is the normal force applied on the ball; F_t is the friction force.

The pH of a water-based solution will have an effect on the potential difference between a steel part and the surrounding liquid, controling the dissolution rate of the metal. As the acidity-basicity of the solution in industrial processes may vary with time, specific corrosion rates are difficult to estimate [5]. The combination of mechanical and electrochemical mechanisms acting simultaneously, known as tribo-corrosion, will cause a higher loss of material than the one produced by the sum of each of the mechanisms acting separately [6].

Erosive (perpendicular stress-impact), abrasive (mostly tangent stress-impact) or sliding (combination of tangent and perpendicular stress-impact) mechanisms acting simultaneously with electrochemical corrosion (produced by local micro-anodes and cathodes) will result in a considerable damage of the equipment, installations and auxiliary elements (stirrers, feeders and valves) [7]. Two types of materials have been used recently in order to reduce this type of wear:

(a) Design of devices with materials highly resistant to electrochemical wear: titanium- or tantalum-based alloys.

(b) Manufacture of parts highly resistant to erosion, abrasion or sliding wear by raising the amount of Mn, Cr, Ni or Mo in both carbon or stainless steels.

In most cases, the first alternative is economically unviable, turning the second one in the most frequently used practice by construction engineering firms dedicated to the design of industrial facilities. Furthermore, this last practice not only raises the mechanical resistance of the material by adding alloying elements but also intrinsically increases resistance to electrochemical corrosion wear [8].

A third alternative to solve tribo-corrosion problems is using a low-cost base (bulk) material and adding a surface with the required chemical and mechanical stability. If the characteristics of the protective surface are adequate (different types of wear may or may not be reduced using HVOF coatings) [9], the chemical-physical and mechanical characteristics of the base material will only demand adequate adherence of this protective layer in order to avoid wear mechanisms. Consequently, it would be detrimental if an inadequate application of the protective surface results in longitudinal (delamination of the layers) or vertical cracks which allow contact between the environment (or corrosive fluid) and the base material [6, 10].

In an HVOF gun oxygen and fuel are combined to produce an extremely high-temperature plasma zone; powder particulates are fed at high speed (~750 m/s) crossing the plasma zone and forming liquid droplets (in the case of metals) or heated ceramic particles. The droplets or particles leave the gun as spray and impact the substrate as splats. The layer produced on the surface may increase in thickness by adding more than one pass (displacement can be achieved by moving the HVOF gun or the substrate) [11].

The combined effect of speed (high kinetic energy) and temperature results in characteristics of a surface layer that simultaneously show low porosity (less than 2%) with very good adherence to the substrate (base metal needing protection) [10, 12].

METHODS

For the sugar industry that uses beets as raw material, protective layers applied with HVOF to auxiliary equipment (valves and rotors) allows very long working periods. In this case, a low-carbon ferritic-perlitic steel, usually required by the construction industry and with 1.0−1.2% Mn, is used as a base for ceramic-metal (cermet) layers: Cr- or W-based carbides. Elemental analysis was made in the samples to identify the proportions in each coating [4].

Three types of coatings were applied to the substrate steel in order to evaluate its performance: a WC + (Co−Cr) layer, a Cr_3C_2 + (Ni−Cr) layer and a combination of these last two. The resulting crystallographic structures of the layers were determined by X-ray diffraction and tribological performance was made by ball-on-disc arrays in a tribology test equipment (Fig. 1). Also, transverse sections were analyzed by SEM microscopy in order to compare porosity, thickness of the layer and adherance to the substrate. Furthermore, the worn out surface produced by the sliding ball was also observed by this technique.

Finally, an industrial comparison between unprotected and protected equipment in a sugar production facility during a 9-month work campaign is presented in order to confirm the effectiveness of this type of layers to prevent tribocorrosion wear.

EXPERIMENTAL

A low-carbon ferritic-pearlitic steel with 1.0−1.2% Mn was used as substrate for three types of layers applied by HVOF with a Sulzer Metco equipment, reaching a 2600 ~ 3100°C temperature at the gun which was separated 0.15 ~ 0.36 m from the steel, using 2−14 kg of powder material per hour resulting in a 500−800 m/s particle speed.

X-ray diffraction patterns were obtained using a Rigaku MiniFlex 600 equipment at 40 kV and 15 mA in a range of 5 to 100 degrees, step of 0.02 degrees and 0.1 degrees per minute angular velocity, in order to obtain smooth and well resolved peaks. Pattern identification was made using PDXL-2 software, with all the peaks identified and labeled.

Tribology tests were made on the three types of layers investigated, using a CETR UMT-2MT universal mechanical tester in order to obtain the friction coefficients by using a WC ball in ball-on-disc tests (Fig. 1). The test had the following parameters: WC ball diameter of 3.175 mm, load applied on the ball of 4 N, test radius of 4.0 mm, linear friction velocity of 0.1 m/s, test duration of 2000 s.

SEM microscopy was made in samples sectioned with a metallographic cutter, and using traditional grinding and polishing techniques. A Hitachi TM3030 microscope was used with 18 kV and different magnifications to characterize the thickness of the layer, distribution of phases inside the layer, porosity inside the layer and adherence to the steel substrate. Also, the worn out surface of the sliding test was observed in the microscope to characterize flattening and fracture (mostly microcracks).

The tribocorrosion performance of this type of layers was evaluated in industrial conditions by comparing a rotor, used in the production of sugar from beets, with and without HVOF protection, specifically the blades of this part, during a 9 month production campaign.

RESULTS AND DISCUSSION

Table 1 indicates the chemical composition of the Cr- and W-based cermets applied with HVOF on a low-alloy steel substrate. Ni, Fe and Co act as binding metal of the carbide particles in order to form ceramic-metal composites, and also assure adherence and toughness at the surface, which may be influenced by the geometry of the part [3]. Though cermets as tool materials for different applications have been extensively studied, the mechanical and corrosive behavior of these layers is considerably different.

Figure 2 shows the identified peaks of the diffraction pattern of the 3 samples investigated. The first sample (Fig. 2a) shows a mixture of WC and $Cr_{23}C_6$, indicating that the metallic Cr particles have chemically reacted with C and formed another carbide during the HVOF layer solidification, while the Co
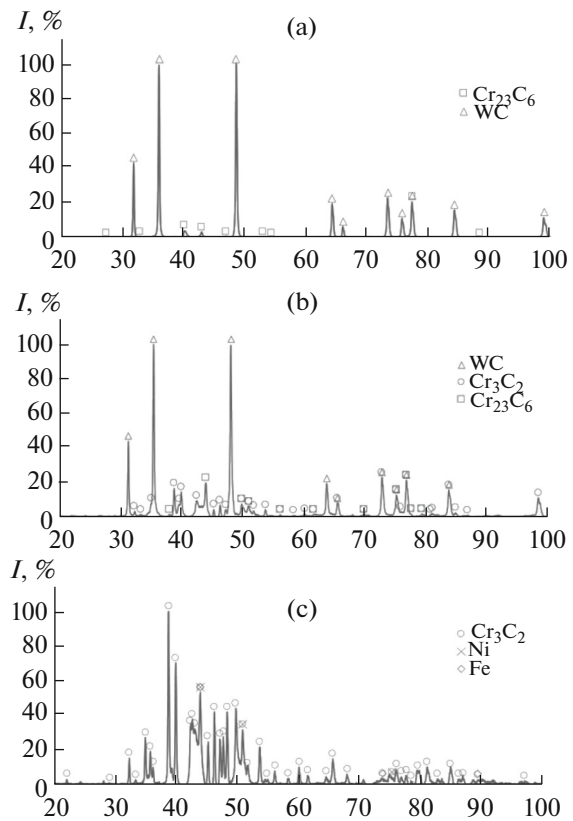

Fig. 2. Peak identification of XRD patterns for sample 1 (a), sample 2 (b) and sample 3 (c).

metallic binder phase peaks are indistinguishable in the pattern, as reported by other authors [13, 14]. Sample 3 (Fig. 2c) is formed by Cr_3C_2 hard particles in a Ni−Fe metallic matrix, though Fe amounts are small and its peaks could correspond to Cr. As expected, sample 2 (Fig. 2b) is formed by a combination of phases present in samples 1 and 3: WC and $Cr_{23}C_6$, on one hand, and Cr_3C_2 on the other, though the combination of these two very different cermet materials makes the identification by XRD of the metallic binder almost impossible.

Results of sliding tribological tests for the three samples are presented in Fig. 3, clearly showing that the WC-based layer has a lower friction coefficient as these carbides are the hardest, while the Cr_3C_2 layer shows both a higher friction coefficient and variations during measurement due to the amount of soft metallic binder present. The combination of both materials (sample 2) has a coefficient, as anticipated, between both values and with moderate variations.

Table 1. Chemical composition for Cr and W based cermets

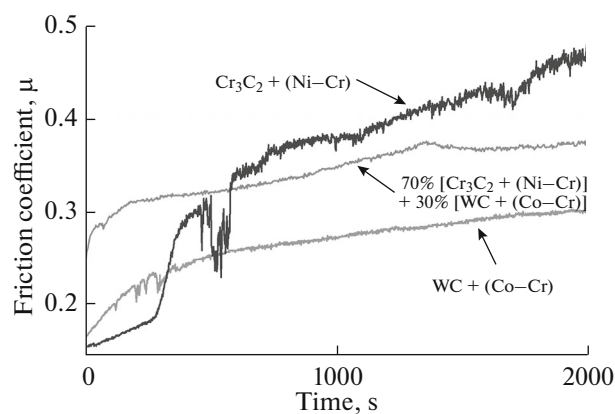| Cr cermet	70% Cr	9.3% C	20.5% Ni	0.2% Fe
W cermet	80% W	5.4% C	10.35% Co	4.25% Cr + Fe

Fig. 3. Friction coefficients vs. time during tribological test for sample 1 (WC + Co−Cr), sample 2 (70% Cr_3C_2-based + 30% WC-based) and sample 3 (Cr_3C_2 + Ni−Cr).
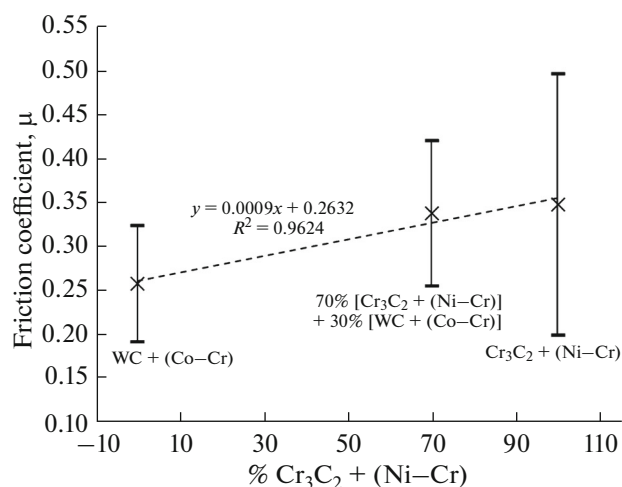

Fig. 4. Friction coefficient vs. chromium cermet amount showing the mean values, as well as minimum and maximum for a 90% confidence level.

If sample 1 is considered to have 0% of Cr_3C_2, Fig. 4 indicates the mean values of the friction coefficient measured by the tribological test as a function of the amount of this constituent, also showing maximum and minimum values obtained during testing (Table 2). As expected, sample 3 (only Cr_3C_2 carbides) shows a high value for the friction coefficient and a considerable variability on this parameter, which may be due to the softness of the layer and the poor adherance between the layer and the substrate. On the other hand, the layers with WC have the smallest variations in the μ values as adherance to the substrate is almost perfect and wear during the test may be limited to one predominant mechanism.

Figures 5 and 6 show the thicknesses, porosity and adherence of the different layers investigated: sample 1 and 3 have a similar thicknesses of ~200 μm, while sample 2 has a thickness of almost half of that value (~100 μm). The most dense layer is the one of sample 3 though it has the lowest adherence to the substrate. The most porous layer is the one from sample 2. Though porosity is present in all samples, the wettabil-

Table 2. Results of tribological test on the layers investigated

Layers	1	2	3
% WC + (Co−Cr)	100	30	0
% Cr_3C_2 + (Ni−Cr)	0	70	100
Mean friction coefficient	0.26	0.34	0.35
Standard deviation	0.04	0.05	0.09
Minimum friction coefficient*	0.33	0.42	0.50
Maximum friction coefficient*	0.19	0.26	0.20

* Considering a 90% confidence level.

ity between Ni and Cr carbides in sample 3 is very good. Yet, adherance between this layer and the steel substrate shows defects (Fig. 6c) as refractoriness of the Cr carbides and their low capacity to maintain temperature during the HVOF process limits diffusion and wettability with Fe-based substrates. When combining the two types of carbides (Fig. 6b), the HVOF process results in splats of either tungsten- or chromium-based carbides which promotes a better wear resistance during sliding as the splats of WC are alternated with chromium carbides.

Feeding two types of powders to the HVOF gun will produce a layer with low porosity though not completely mixed (Fig. 6b): zones of WC are observed in white and the Cr carbides and Ni phase in gray and in a larger amount. The phase that contains Ni may be considered as a continuous matrix with WC isolated zones, as the combination of Cr−C−Ni will produce an eutectic phase (approximately 1255°C) [15] that promotes densification and adherence to the substrate. As expected, layers produced by HVOF have a certain level of porosity [16] as observed in Fig. 6.

If the wear produced by the sliding ball is compared between samples 1 and 3 (Fig. 7a, 7c), evident differences include the following: the WC-based layer (Fig. 7a) is considerably harder and though small zones are flattened out, variations in height are observed as well as a large amount of microcracks, due to the intrinsic low toughness of the material. On the other hand, sample 3 (Fig. 7c) shows a more uniform surface with larger and deeper cracks along with spalling [17] as a result of adherance wear. The combination of both carbides in one layer (Fig. 7b) results in less flattening, moderate spalling and pull-out zones [18].

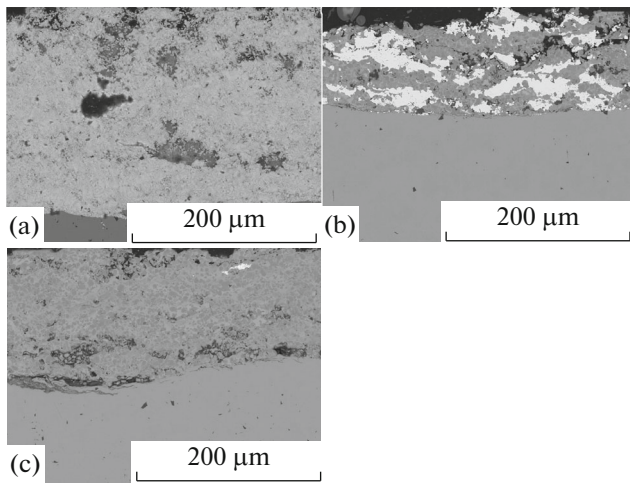In all samples (Fig. 7) evidence of both abrasive and adhesive wear is observed, though pull-out mech-

Fig. 5. SEM micrographs showing the thickness of the layer for samples 1 (a), 2 (b) and 3 (c). Lower part of the images correspond to steel substrate.
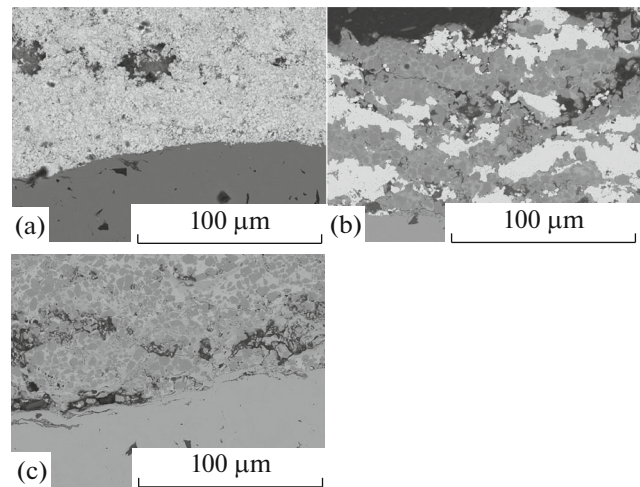

Fig. 6. SEM micrographs showing at high magnification (1000×) the porosity and adherence of the layer for samples 1 (a), 2 (b) and 3 (c).

anisms are more pronounced in sample 1 as the plasticity of the Ni binder in sample 3 [19] as well as the Cr_3C_2 carbides are more effective in reducing this type of wear [17]. All the layers are dense enough to prevent delamination during sliding tests [11].

Cracks in Fig. 7c seem to advance both through the binder as well as fracturing carbide grains, while the low fracture toughness of the WC layer (Fig. 7a) seem to achieve crack propagation by the growth of microcracks.

Though WC-based layers applied by HVOF have been reported to form W_2C (or W_xC_y-type [14]) due to decarburization [20, 21], resulting in lower mechanical adherance and toughness, the use of Co−Cr binders prevent the formation of these decarburized particles, due the chemical stability provided by the Cr_3C_2 carbides, which also improve corrosion resistance [16]. Figure 2a, 2b confirm that sample 1 has not suffered decarburization as W_2C phase is not present and Cr_3C_2 is. Also, no evidence of amorphous phase formation was detected as reported by other authors [13, 18].

After a nine month working campaign, the effect of wear in a rotating auxiliary system, used in the production of sugar, is shown in Figs. 8, 9. The material of the part shown in Fig. 8 is a rotor structure damaged with grooves or tracks over the surface of a hot rolled steel with a ferrite-pearlite structure (0.30% C and 1.20% Mn). On the other hand, Fig. 9 presents the surface integrity, at the end of the campaign, of the same steel with a 200 μm layer applied with HVOF formed by different proportions of tungsten- and chromium-based layers at different zones of the part, as industrial experience and cost efficiency dictate the use of harder and more expensive cermets only on the zones subject to higher wear. In both situations, the material was in contact with an alkaline solution formed with different

proportions of solids in suspension (siliceous clays) for a nine month period, at a temperature of 60°C.

The surface wear of the part shown in Fig. 9 is almost non-existent, though at many zones the thickness of the protecting layer has been reduced to half (~100 μm).

Though kinetic and thermodynamical models have been proposed in order to understand the effect of changing process parameters such as fuel flow rate, powder velocity, nozzle temperature and spray distance [22], the amount of variables (including geometry and gun/substrate relative movement to insure uniform thickness) results, in most cases, in trial and error and/or best practices procedures to protect industrial parts subject to wear (Fig. 8).
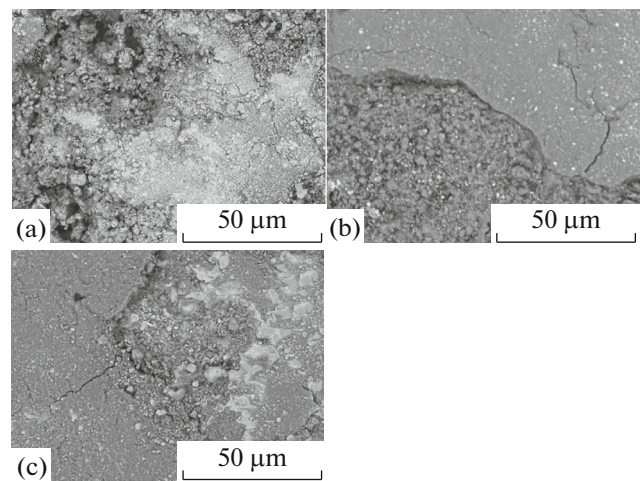

Fig. 7. SEM micrographs of the worn out surface after ball-on disc tests for samples 1 (a), 2 (b) and 3 (c).
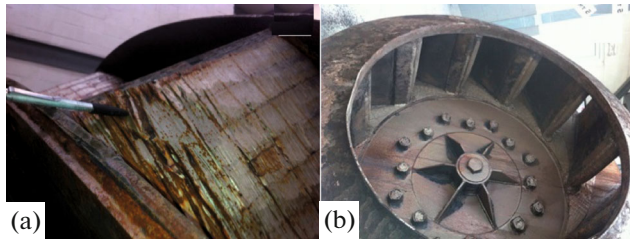
Fig. 8. Final state of a rotor after a working campaign in a sugar production facility.
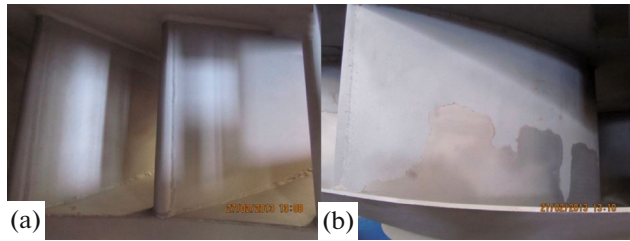

Fig. 9. Final state of a Cr and W cermet layers protected rotor after a working campaign in a sugar production facility.

CONCLUSIONS

HVOF projection technique is a very efficient surface treatment, especially in those cases where auxiliary equipment (rotors, valves or pumps) must be protected from wear in sugar production facilities that use beet.

The use this type of protective layers is both structural and economically efficient, as it allows for the same equipment to be used for longer periods of time, reducing maintenance or repairing costs. Parts not protected with HVOF layers can suffer damage that will make its further recovery (for example, by applying welded metal layers) impossible.

WC−Co−Cr HVOF layers are capable protections against wear, but their combination with Cr_3C_2−Ni−Cr is cheaper and also efficient in protecting zones subject to low abrasion, though it is porous and not homogeneous.

The use of Cr_3C_2 results in higher variability of the friction coefficient due to its low and uneven adherance to the substrate (and not because of the density of the layer itself).

ACKNOWLEDGMENTS

REFERENCES

1. Siegmann, St., Brandt, O., and Margadant, N., *Proc. 1st Int. Thermal Spray Conference "Thermal Spray: Surface Engineering",* Montreal, 2000.

2. Yunus, M. and Rahman, J.F., *Int. J. Adv. Eng. Sci. Technol.,* 2011, vol. 10, p. 275.

3. El Rayes, M.M., Abdo, H.S., and Khalil, A.K., *Int. J. Electrochem. Sci.,* 2013, vol. 8, p. 1117.

4. Verdeja, L.F., Sancho, J.P., Ballester, A., and Gonzalez, R., *Refractory and Ceramic Materials,* Madrid: Syntesis, 2014.

5. Ballester, A., Verdeja, L.F., and Sancho, J.P., *Metalurgia Extractiva: Fundamentos,* Madrid: Syntesis, 2000, p. 219.

6. Vazquez, A. and Damborenea, J.J., *Ciencia e Ingenierya de las Superficies de los Materiales Metalicos,* Madrid: CSIC, 2000, p. 9.

7. Kumari, K., Anand, K., Bellacci, M., and Giannozzi, M., *Wear,* 2010, vol. 268, p. 1309.

8. Kap, I., Starostin, M., Shter, G.E., and Grader, G.S., *Mater. Corros.,* 2012, vol. 63, p. 571.

9. *Introduction to Thermal Spray Processing. Handbook of Thermal Spray Technology,* Davis, J.R., Ed., Materials Park, OH: ASM Int., 2004, p. 3.

10. Puertolas, J.A., Ryos, R., Castro, M., and Casals, J.M., *Tecnologya de Superficies en Materiales,* Madrid: Syntesis, 2010, p. 155.

11. Bolelli, G., Lusvarghi, L., and Barletta, M., *Wear,* 2009, vol. 267, p. 944.

12. Sobolev, V.V., Guilemany, J.M., and Nutting, J., *High Velocity Oxy-Fuel Spraying,* London: Maney Publ., Inst. of Metals, 2004.

13. Sahraoui, T., Fenineche, N., Montavon, G., and Coddet, C., *Mater. Des.,* 2003, vol. 24, p. 309.

14. Babilius, A., *Mater. Sci.,* 2003, vol. 9, p. 183.

15. Bolelli, G., Berge, L.M., Bonetti, M., and Lusvarghi, L., *Wear,* 2014, vol. 309, p. 96.

16. Wang, L.J., Qiu, P.X., Liu, Y., et al., *Trans. Nonferrous Met. Soc. China,* 2013, vol. 23, p. 2611.

17. Shukla, V., Jayaganthan, R., and Tewari, V., *Int. J. Surf. Eng. Interdiscip. Mater. Sci.*, 2014, vol. 4, p. 44.

18. Picas, J.A., Xiong, Y., Punset, M., et al., *Int. J. Refract. Met. Hard Mater.,* 2009, vol. 27, p. 344.

19. Brezinova, J., Guzanova, A., Draganovska, D., and Egri, M., *Acta Mech. Automat.,* 2013, vol. 7, p. 135.

20. Kailash, S., Praveen, A., Suresh, S. et al., *Int. J. ChemTech Res.,* 2014, vol. 6, p. 3346.

21. Guilemany, J.M., de Paco, J.M., Nutting, J., and Miguel, J.R., *Metall. Mater. Trans. A,* 1999, vol. 30, p. 1913.

22. Cheng, D., Xu, Q., Trapaga, G., and Lavernia, E., *Metall. Mater. Trans. A,* 2001, vol. 32, p. 1609.